Composites Science and Technology 135 (2016) 28–38

Contents lists available at ScienceDirect

Composites Science and Technology

journal homepage: http://www.elsevier.com/locate/compscitech

# Improved mechanical properties of carbon fiber/graphene oxide-epoxy hybrid composites

Abhishek K. Pathak [a, b], Munu Borah [a, b], Ashish Gupta [a, b], T. Yokozeki [c], Sanjay R. Dhakate [a, b, *]

[a] Advanced Carbon Products Section, Advanced Materials and Devices Division, CSIR-National Physical Laboratory, Dr. K.S. Krishnan Marg, New Delhi 110012, India
[b] Academy of Scientific Innovation and Research (AcSIR), NPL, New Delhi, India
[c] Department of Aeronautics and Astronautics, Graduate School of Engineering, The University of Tokyo, Tokyo, Japan

ARTICLE INFO

*Article history:*
Received 27 May 2016
Received in revised form
6 September 2016
Accepted 7 September 2016
Available online 8 September 2016

*Keywords:*
Carbon fibers
Hybrid composites
Photoelectron spectroscopy
Mechanical properties

ABSTRACT

The mechanical properties of carbon fiber reinforced polymer composites depend upon fiber-matrix interfacial properties. In this investigation to improve the mechanical properties of polymer composites, graphene oxide was used as one of the filler for the development of carbon fiber/graphene oxide-epoxy hybrid composites. Initially, epoxy resin was modified by incorporating different weight% of graphene oxide from 0.1 to 0.6 wt%. The desired size of carbon fiber fabric was impregnated with modified epoxy resin to develop hybrid composites by compression molding technique. The graphene oxide synthesized was characterized by various techniques such as FTIR, XPS, NMR, XRD and Raman Spectroscopy. It is observed that graphene oxide synthesized possesses different type of functional groups which are responsible for making interactions with epoxy resin and Carbon fibers. The hybrid composite flexural strength increases by 66%, flexural modulus by 72%, while interlaminar shear strength (ILSS) increases by 25% at 0.3 wt% of graphene oxide included in the carbon fiber reinforced polymer hybrid composites. The enhancement in the properties of composites at the percolation threshold of graphene oxide is due to hydrogen type bonding and mechanical interlocking of graphene oxide with carbon fibers and epoxy resin. The graphene oxide utilization is one of the approaches for improving the properties of carbon fiber polymer composites.



## 1. Introduction

Carbon fiber reinforced polymer composites have been extensively used in a wide range of applications such as aerospace, automotive, wind energy, marine turbine blades and sports sector because of their superior strength to weight, high thermal stability and excellent corrosion resistance [1,2]. Their low fabrication cost, ease of handling and fatigue damage resistance owe to metal counterpart in various applications [3–5]. In the composites, fiber plays an important role as load bearing component and polymer matrix provides back support to fiber by maintaining its orientation into the composites. The fiber volume content is essentially dominated the mechanical properties of unidirectional carbon fiber polymer matrix composite. In the laminated composites, carbon fiber is mainly responsible for high in-plane mechanical properties, whereas polymer matrix is mainly for out of plane properties.

The carbon fiber laminated composites are extremely capable to crack initiation and propagation through various modes of failure [6,7]. The delamination is one of the major crack growth mode, which causes critical depression in in-plane strength and stiffness [8,9]. Another problem is the surface inertness of carbon fiber which exhibits poor interfacial interactions with polymer matrix [10]. All above drawbacks are potentially led to catastrophic failure of the whole composite structure. In this direction several techniques have been introduced to improve mechanical properties (in-plane and out of plane) such as Z pinning [11], stitching of fiber [12], designing 3D fabric design [13], fiber surface modification [14–16] and matrix modifications [17–19] etc. These modification methods have been reported with improved inter-laminar mechanical properties at high complexity and cost. Traditionally, matrix

* Corresponding author. Advanced Carbon Products Section, Advanced Materials and Devices Division, CSIR-National Physical Laboratory, Dr. K.S. Krishnan Marg, New Delhi 110012, India.
*E-mail address:* dhakate@mail.nplindia.org (S.R. Dhakate).

http://dx.doi.org/10.1016/j.compscitech.2016.09.007
0266-3538/

modification is relatively easy and cost effective procedure without compromising other mechanical and structural properties of composite.

It is reported that improvement in mechanical properties of composites using matrix modification depends largely on the interface to volume ratio and filler size [20,21]. So in this direction nanofillers are playing important role for the modification in polymer matrix. Some of the work has been already reported on the modifications of composite interface by reinforcing mechanism. The modification combines effect was explained from a variety of interface theories such as chemical bonding [22], wetting, mechanical interlock [23] and local stiffness of polymer matrix [24]. In this area, enhancement in mechanical properties of composites has been reported by incorporating nanoscale fillers such as CNT [25–27], fullerenes [28,29] and nanoclay [30,31]. Ogasawara et al. has reported 60% enhancement in interleminar fracture toughness by incorporating fullerene (0.1–1 wt%) in the matrix resin [28]. On the other hand Vaganov et al. examined the enhancement of 40% in fracture toughness by incorporating 1.0 wt% CNT in epoxy/carbon fiber composites [32]. Also, Xua et al. [31] have reported significant improvement of flexural properties using clay-reinforced epoxy/carbon fiber composite.

Recently, graphene filled composites have been widely investigated due to the outstanding electrical, thermal and mechanical properties of graphene. Over the past few years, incorporation of graphene or graphene oxide (GO) sheets has been reported on a wide range of polymer matrix [33–38]. In pursuance of achieving optimum enhancement in mechanical properties of polymer matrix composites, there are many key issues should be fixed, i.e., dispersion and alignment of graphene in the polymer and surface modification of graphene for favorable interaction. It is well known, synthesis of graphene produced in entangled structure and interlaminar van der Waal forces promote agglomeration of the graphene sheet. Consequently, the dispersion and exfoliation of graphene in media is great obstacle when it mixed with polymer. The poor dispersion and agglomeration of graphene sheet created nano defects in laminated composites which causes only minimal enhancement mechanical properties. To control the above shortage, excellent approaches have been tackled to covalent functionalization of graphite sheet from oxidation method to improve their affinity with polymer matrix. The oxidative form of graphite sheet, i.e., graphene oxide plays a very important role as nano filler for matrix modification. Its surface and edge oxygen functional groups provide an ambient path for strong binding with polymer matrix. Its high dispersion ability and strong interlocking with polymer matrix commits potentially effective reinforcement in polymer composites. In this respect Zhang et al. reported the 70.9% and 36.9% improvement in interfacial shear strength (IFSS) of virgin carbon fiber and commercial sizing carbon fiber composites by incorporating 5.0 wt% GO [39].

In the present studies, we have introduced graphene oxide into the polymer matrix using very conventional method i.e., wet transfer process. The GO-epoxy resin was used for development of carbon fiber hybrid composites and effect of GO content on bending properties of composites was investigated. We are reporting improvement in bending strength and ILSS by including different weight of GO into the epoxy/carbon fiber hybrid composites.

## 2. Materials and experimental section

### 2.1. Materials

Natural Graphite procured from Pure Carbon, Pune, India. Sodium nitrate (99.98% pure) and potassium permanganate (99% pure) were all from Thermo Fisher Scientific India Pvt. Ltd., Mumbai. $H_2SO_4$ (98% v/v), HCl (35% v/v) and $H_2O_2$ (30% v/v) were obtained from Thomas Baker Pvt. Ltd. Mumbai, Merck Specialties Pvt. Ltd. Mumbai and RFCL limited Gujarat respectively. All the chemicals were used without further purifications. T-300 carbon fiber fabric procured from Ram Composite Products, Hyderabad. Epoxy resin LY556 and hardener Triethylenetetramine (TETA) procured from Huntsman, USA and central drug house, India respectively.

### 2.2. Synthesis of graphene oxide

Graphene oxide was synthesized by the Hummer's method followed by an appropriate washing process for better purity [40,41]. Water free solution of graphite flakes (5 g) and sodium nitrate (2.5 g) in sulfuric acid (150 ml) was prepared. Potassium permanganate (15 g) slowly added to the water free mixture while stirring and maintained temperature 10–15 °C by keeping reaction system in ice bath. The mixture was stirred slowly for 24 h at 40 °C and to achieve a uniform oxidation reaction. Later on the temperature increased to 100 °C for high rate of oxidation for 1 h and then added 250 ml of distilled water in the reaction mixture and stirred for 1 h. Finally 15 ml 30% hydrogen peroxide mixed to reaction mixture to stop the reaction and diluted with 500 ml distilled water. Solution was filtered and washed with distilled water until the pH value of supernatant reached to 5–6. To obtain pure GO, resulting GO suspension were washed with 5% HCl solution to remove unreacted potassium permanganate and metal impurities, followed by washing with distilled water to separate chloride ions and acid. GO flakes were obtained by drying washed GO in oven at 60 °C for 24 h.

### 2.3. Preparation of GO reinforced carbon fiber/epoxy composites

The epoxy resin was modified by introducing GO via wet transfer. The GO was dispersed in ethanol solution by ultrasonically for 2 h and then mixed with epoxy resin. The excess ethanol from a GO-epoxy mixture was removed by keeping mixture in oven at temperature 60 °C. Later on mixture was stirred for 24 h at 50 °C to get a homogeneous mixture. The epoxy resin was modified by incorporating different wt% of GO from 0.1 to 0.6 wt%. The desired size of carbon fiber fabric was impregnated with epoxy-GO mixture to get prepreg. The prepreg was kept in a vacuum oven to remove entrap air. The desired number of prepreg was arranged on a metallic plate and then kept on the hot plate of hydraulic press. The pressure was applied at temperature 90 °C to get desired hybrid composites. The processing of hybrid composite schematically depicted in Fig. 1.

### 2.4. Characterization of the GO and GO/epoxy carbon fiber hybrid composites

The surface morphology of GO flakes, dispersed GO and fractured surface of GO reinforced hybrid composite was recorded by Scanning Electron Microscopy (Vi-EVO, MA-10, Carl-Zeiss, UK). Samples were coated with gold using sputtering coater before observing the morphology. The prepared GO was characterized by Transmission Electron Microscope (JEOL model JEM 2100, Japan). Sample for TEM study was prepared by dispersing a requisite amount of GO in a known quantity of Milli-Q water by ultrasonication for 1 h. A drop of the sample was placed on a lacey carbon film on a copper grid and was allowed to dry at room temperature for 24 h. The surface chemical analysis, relative elemental composition and electronic state of GO was recorded using Multi Lab 2000 spectrometer (Thermo Electron Corporation, England) with Al Kα as an X-ray source with radiation energy

1485.6 eV. All the measurements were run through 14.9 keV anode voltages, a 4.6 Å filament current and a 20 mA emission current. The XPS survey spectra were obtained with 50 eV pass energy with 1.0 eV step size. Core level spectra were obtained at 50 eV pass energy with a 0.10 eV step size.

The crystallographic analysis of GO was analyzed using X-ray diffractometer (D–8 Advanced Bruker powder X-ray diffractometer) using CuKα radiation (λ = 1.5418 Å) at a scanning rate of 1°/min with voltage 40 kV with a current of 40 mA within range of 2θ = 5°–60°. Functional groups present on GO prepared by the Hummer's method were confirmed by Fourier Transform Infrared Spectrometer (Perkin Elmer, Model: Spectrum GX FT-IR system). The sample was mixed with KBr powder (Sigma Aldrich) and the resultant mixture was pressed to form a palette (circular disk). The spectrum was recorded within the range of 4000 $cm^{-1}$- 400 $cm^{-1}$ averaging 10 scans with 1 $cm^{-1}$ interval and at a resolution of 4 $cm^{-1}$. GO was characterized by $^{13}C$- Solid State Nuclear Magnetic Resonance (NMR) spectroscopy to get information of carbon states in prepared GO (ECX-400 JEOL-400 MHz high resolution multinuclear FT-NMR spectrometer for solid). Spectrum was recorded with single pulse experiment at full range peak picking and noise factor 5. The Raman spectrum of GO was recorded using Reninshaw Raman Spectrometer (Micro Raman model-Invia reflex) with 514 nm laser excitation. For Raman Spectra 50× objective lens was used with laser power 5 mW (laser spot size -0.8 μm).

The mechanical properties of composite were measured using Instron Universal Testing machine model 5967. Samples for testing were prepared according to ASTM D 790 standards. The bending strength measured on a sample of length 80.00 mm, width 15.00 mm and thickness 2.00 mm by three point bending technique at the cross head speed 1 mm/min. The density (ρ) of GO based carbon fiber/epoxy composite was calculated using the equation: ρ = m/v, where, m is the weight of the composite and v is the volume of the composite. The interleminar shear strength (ILSS) of composite samples was calculated using the relationship:

$$F = 0.75 * P/b * h \quad (1)$$

Where F is the short-beam strength (MPa), P is the maximum load (N) experienced by specimen, b is measured width (mm) and h is the measured thickness (mm) of composite specimen. Samples for ILSS were prepared according to ASTM D2344 standard.

## 3. Results and discussion

### 3.1. Characterizations of the GO

Functional groups present on the surface of GO was evaluated by FTIR and it is depicted in Fig. 2. The peak at 1735.59 $cm^{-1}$ is attributed to stretching vibration of carbonyl group part of a carboxylic acid. Peaks at 1639.41 $cm^{-1}$, 1463.32 $cm^{-1}$ and 1127.45 $cm^{-1}$ corresponds to the stretching vibration of C=C, C–OH and C–O respectively. 1264.27 $cm^{-1}$ and 1028.22 $cm^{-1}$ peaks indicating symmetric and asymmetric stretching vibrations of epoxy ring (C–O–C) respectively [42,43].

$^{13}C$ NMR or Carbon-NMR is very important tool for structure elucidation of the organic compounds. This technique allows the identification of different state of carbon atom in organic

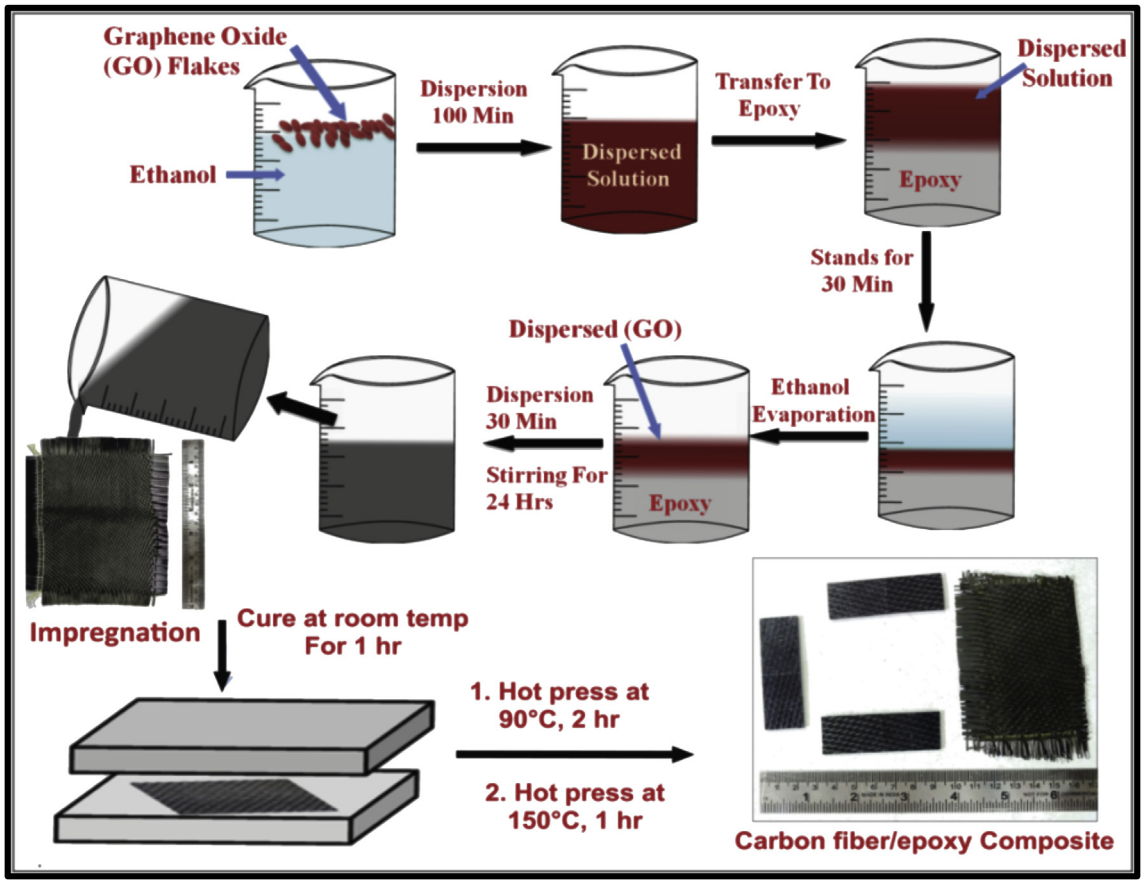


**Fig. 1.** Schematic diagram of introduction of GO into epoxy matrix to form GO reinforced epoxy-carbon fiber hybrid composites.

molecules. The single pulse $^{13}C$ NMR spectrum of graphene oxide has shown in Fig. 3. The $^{13}C$- Solid NMR of GO resulted in four major peaks with chemical shift at 60.07 ppm, 70.42 ppm, 135.01 ppm and 169.66 ppm confirming the function group C–O–C (epoxy), C–OH (hydroxyl), C=C (conjugated $sp^2$) and HO–C=O (carboxylic) respectively [42–45]. Peak intensities of all functional groups attributed to the concentration of that nucleus in samples. So the epoxy group has high intensity among other functional groups, indicating maximum number of carbon nucleus with that group. Additionally, carbon attached to hydroxyl group has recorded with second highest peak. Also the C=C bond intensity is lower because of a breakdown in conjugation due to oxygen based functional group. Lower number of carboxylic acid group attributing lowest intensity of it in GO.

The XRD spectrum of the natural graphite and graphite oxide were recorded in the study of crystalline nature along with phase purity in the natural graphite to graphite oxide during the chemical oxidation reaction. The XRD pattern of natural graphite shows a diffraction peak at $2\theta = 26.59^\circ$ for its (002) plane and this peak disappeared after oxidation of graphite into graphene oxide (Fig. 4). The appearance of new diffraction peak at $2\theta = 10.18^\circ$ which is corresponding to (002) plane of GO [46]. The interlayer spacing of natural graphite and GO were calculated according to Bragg's law of diffraction:

$$N\lambda = 2d \sin\theta \quad (2)$$

Where $\lambda$ is the wavelength of X-ray used, N is diffraction order and d is interlayer space.

The calculated value of interlayer spacing of GO is $d_{002} = 8.71$ Å whereas in case of natural graphite it is $d_{002} = 3.35$ Å which is less and it is half of d-spacing of GO. The larger d-spacing of GO suggested that the level of oxidation in graphite lattice. Various oxygen based functional groups onto the surface are responsible for many defects or nanoholes in GO and consequent lattice distortion of graphite lattice. GO peak intensity is lower than graphite which demonstrating the disorder structure of GO also a sharp peak of graphite indicating that graphite is composed from well-ordered graphene sheets [43,47]. Also, it is observed that peak at 20.6° is the second order peak of GO which is absent in case of graphite.

The reinforcing filler or additive material used in the development of fiber reinforced polymer composites possesses functional groups on their surface. These groups generally are responsible for interaction or bonding between reinforcing and the polymeric matrix. The XPS is an excellent tool to identify the functional groups present on the surface reinforcing additives in the quantitative amount. Fig. 5(a) and (b) are showing the de-convolution of XPS spectra of GO for carbon and oxygen respectively.

The C1s and O1s spectra involve the electron transition from carbon–oxygen atoms of different atomic configurations; and their shape depends upon atomic densities. The evaluation of bonding content consists of spectra background subtraction, followed by the fitting of Gaussian–Lorentzian asymmetric functions to the measured spectra, selecting the relevant binding energy values from literature [48,49]. In both the cases, asymmetric peaks are observed centered at different binding energies with long tail extended to the higher energy region. The deconvolution of Cls spectra is splitting into four peaks, (1) carbon in graphitic type (C–C/C=C), (2) carbon singly bound to oxygen (C–O) in phenols and epoxy (C–OH/C–O–C), (3) carbon doubly bound to oxygen (C=O) in ketones and quinines and (4) carbon bound to two oxygen (–COO) carboxylic acid. The deconvolution of the O1s spectrum results in two peaks (Fig. 5(b)), (1) oxygen single bound to carbon (C–OH/C–O–C) in the form of hydroxyl/epoxy and (2) oxygen doubly bound to carbon (C=O) in the form (C=O/HO–C=O) carbonyl group or carboxylic. The integrated area involves under peak designate the bond intensity of assigned bond. Greater area under curve possesses higher bond intensity of that bond which is directly linked with its number of bond present in that molecule. Table 1 is comparing the binding energies of C1s and O1s deconvoluted peak of different functional group present on the surface of graphene oxide.

Raman spectroscopy is an important non-destructive technique for structure elucidation of carbon based materials [50]. Highly ordered graphite sheet has only couples of high intense Raman-active bands, the vibration because of in-phase graphite lattice (G band) appeared at 1579.53 $cm^{-1}$ due to 1st order scattering of the $E_{2g}$ mode [51] and small band (D band) appeared at 1350.96 $cm^{-1}$ (in Fig. 6(a)), this is due to the presence of defects. This occurs due to the surface modification by oxidation reaction in the graphite material such as bond length, bond angle, edge and vacancy defects etc. Also the presence of a 2D band (or G′ band) at 2720.24 $cm^{-1}$ is the result of overtone of D-band and this band is used to elucidate structure in c-axis orientation [52].

In case of Raman spectra of GO, G-band shifted at higher frequency 1598.83 $cm^{-1}$ because of oxidation of graphite and D-band

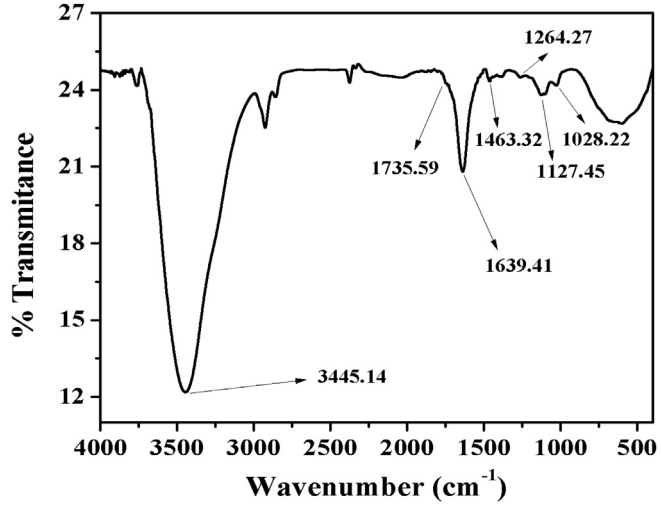


**Fig. 2.** FT-IR plot of graphene oxide (GO).

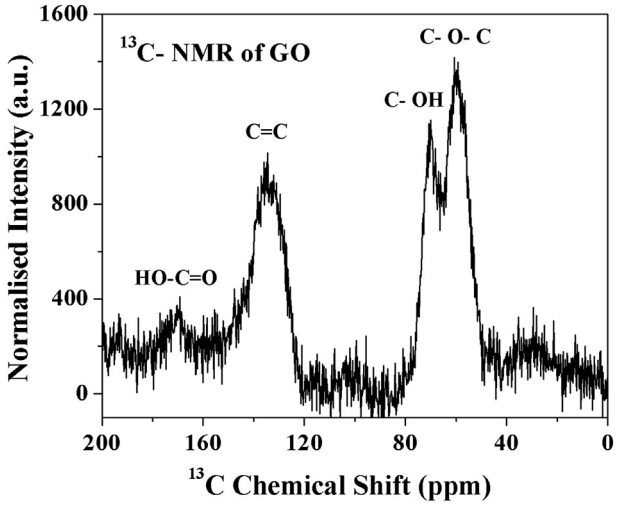


**Fig. 3.** $^{13}C$ NMR plot of graphene oxide (GO).

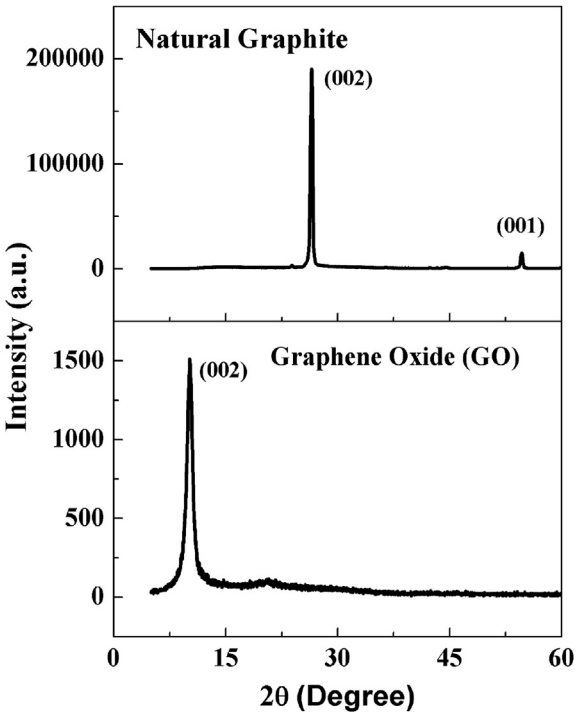


**Fig. 4.** XRD plot of Graphene oxide (GO) relative to natural graphite flakes.

appeared at 1351.01 $cm^{-1}$ with higher intensity. The shift in G-band arises because of the increase in the number of $sp^3$ carbons due to oxidation whereas the intense D-peak is a result of imperfection created as a consequence of in plane hetero-atom oxygen based functional group on the graphitic basal plane.

The $I_D/I_G$ ratio of natural graphite and GO is 0.21 and 0.97 respectively. This increment in $I_D/I_G$ from natural graphite to GO as a result of disorder carbon on the surface modification of graphite and loss of conjugation of carbon-carbon double bond along with size of $sp^2$ ring on the GO basal plane indicating the increase in disorder after oxidation. On the other hands, above Fig. 6(b) has two more low intensity peaks at 2708.30 $cm^{-1}$ and 2937.26 $cm^{-1}$ which is corresponding 2D and (D + G) peak respectively. The reductions in intensity of a 2D band of GO associated with the breaking of stacking order because of oxidation reaction.

**Table 1**
Functional groups present on surface of GO evaluated by XPS curve fitting.

| | Assignment | BE [eV] | Integrated area |
|---|---|---|---|
| Peak 1 (C1s) | C–C/C=C | 283.74 | 10797.10 |
| Peak 2(C1s) | C–OH/C–O–C | 286.14 | 28093.20 |
| Peak 3(C1s) | C=O | 288.24 | 17403.70 |
| Peak 4 (C1s) | O=C–OH | 289.38 | 11208.20 |
| Peak 1(O1s) | C–OH/C–O–C | 530.17 | 16753.77 |
| Peak 2(O1s) | C=O/HO–C=O | 533.73 | 39443.80 |

### 3.2. Morphological and crystallinity analysis of GO

Fig. 7 showing the SEM images of GO and dispersed GO. It is observed the wrinkled GO or the folded GO sheets in Fig. 7(a). It can easily conclude by seeing the image 7(a) that GO contain few number of layers of graphene. In Fig. 7(b), SEM image of GO after dispersion in organic solvent, the size of GO sheet is calculated using SEM image and it varies from 2 to 7 μm. The dispersed GO sheets are introduced in epoxy resin (Fig. 7(c)) and size of dispersed GO sheets in epoxy composite is almost similar to dispersed GO depicted in Fig. 7(b) after wet transfer. Also GO have tendency of agglomeration at higher concentration in epoxy resin (white circle marked in Fig. 7(d)).

The surface morphological and crystalline behavior of synthesized GO were analyzed using TEM and selected area electron diffraction (SAED) pattern as represented in Fig. 8. The of GO in Fig. 8(c) shows semi transparent sheet of few layers of GO along with wrinkle structures, this confirms few layer GO as shown in Fig. 8(a) and (b) after ultrasonication. Since these samples processed under strong oxidation and as a consequence in high amounts of oxygenated functional groups on the surface and edge of sheet, because of it GO flakes are suitable for exfoliation into a few layers after ultrasonication. Fig. 8(a) confirmed the few layer of GO and reveals that few layer of GO sheet having interlayer spacing of 0.35 nm. The selected area diffraction (SEAD) of GO sample is showing the 6 member ring pattern in an identical manner as expected for graphitic material.

The SAED pattern is one of the important and efficient tool uses to analyze the crystalline nature of nano materials. The SEAD pattern of the synthesized GO sample has shown in Fig. 8(d). It is revealed that the SAED pattern of a GO sample show distinct diffraction spot with a six fold pattern that implies with its hexagonal lattice [43]. This pattern of our synthesized GO closely matched with other GO sample recorder by other research groups [53]. The SAED pattern of GO concluded that GO is not only composed from fully amorphous regions, but also include

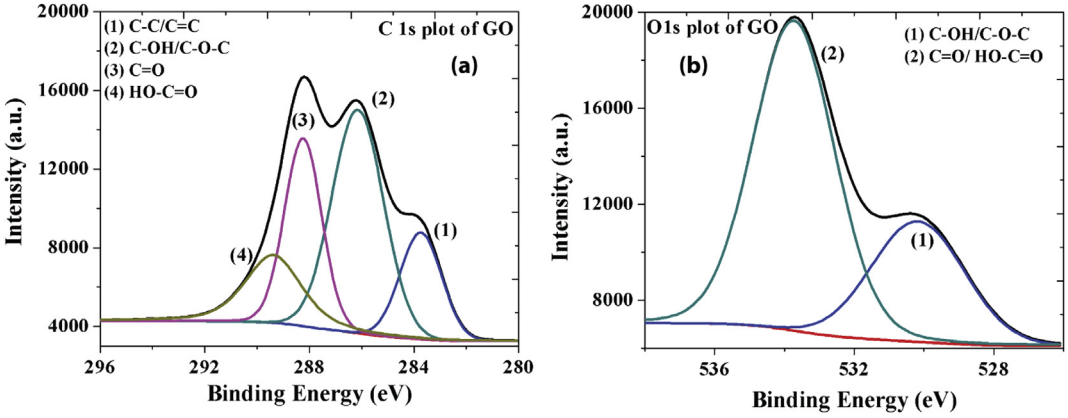


**Fig. 5.** XPS deconvoluted spectra of GO (a) C1s peak and (b) O1s peak.

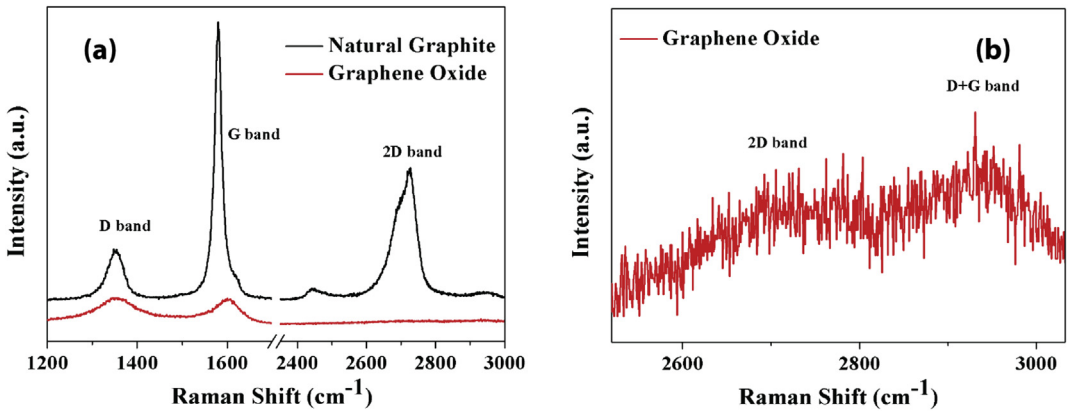


**Fig. 6.** Compares the Raman spectrum of (a) Natural Graphite and GO and (b) zoom image of GO in the range of 2500–3000 $cm^{-1}$.

crystalline regions [54].

### 3.3. Mechanical properties of composites

In the case of carbon fiber-epoxy composite flexural failure is limited by fibers, in Fig. 11(a) depicted variation in flexural strength with increasing the GO content in epoxy matrix hybrid polymer composites. Initially, flexural strength of the carbon fiber polymer composites with fiber content 45 ± 2 wt% is 425 MPa. While after GO addition in epoxy resin and composites developed there from shows upward trend in mechanical properties. At 0.1 wt% of GO content, flexural strength increases to 509 MPa and it reaches a maximum up to 710 MPa at 0.3 wt% GO. After 0.3 wt% GO strength decreases continuously and the resultant value is higher as compare to composite without GO i.e., 508 MPa. Also, it is important to note that the deviation in strength is higher after 0.2 wt% of GO in composites. This clearly brings out the fact that the addition of GO is helpful in improving the mechanical properties of carbon fiber epoxy composites. The increase in strength can be results of interfacial bond created between the fiber and epoxy matrix via GO. As investigated by various techniques represented in Figs. 2–5 (FTIR, $^{13}C$ NMR, XRD and XPS respectively), the GO surface present functional groups C–O–C (epoxy), C–OH (hydroxyl), C=C (conjugated $sp^2$) and HO–C=O (carboxylic).

Dhakate et al. reported in earlier study carbon fiber possesses the phenolic/hydroxyl, carbonyl and carboxylic as well as some nitrogen containing functional group on the surface fibers [55]. The functional group present on graphene oxide can form interactions with both functional groups of carbon fibers and epoxy resin. Thus the strong interaction attributed to decrease in elongation as

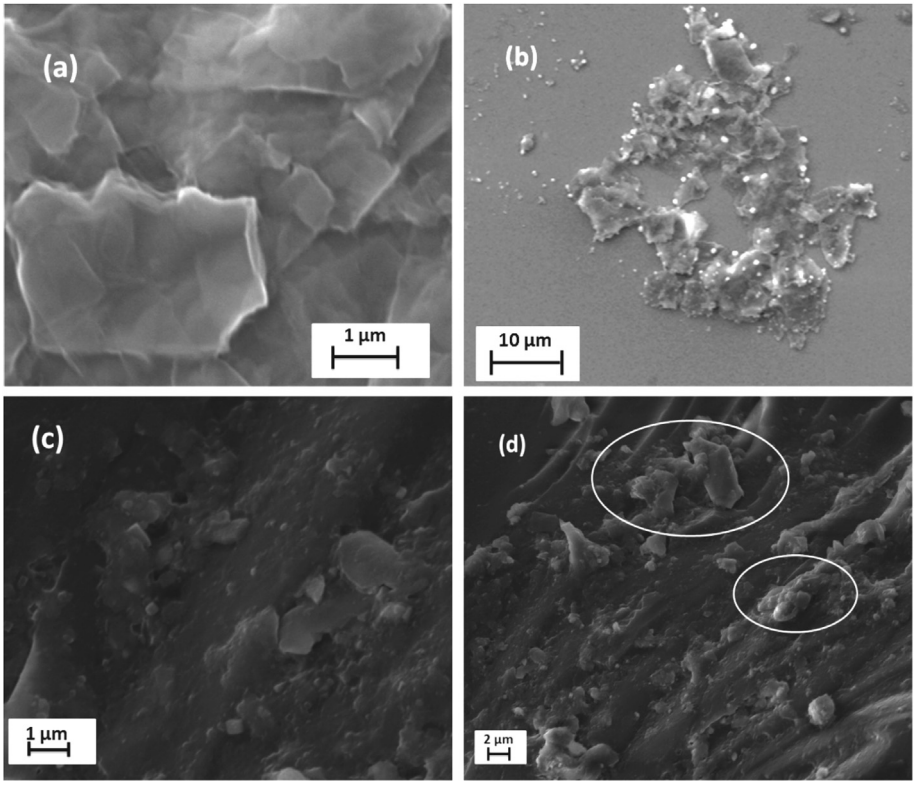


**Fig. 7.** SEM images of (a) GO flakes (b) dispersed GO sheet (c) disperse GO sheets in epoxy polymer and (d) agglomeration of GO into the epoxy resin.

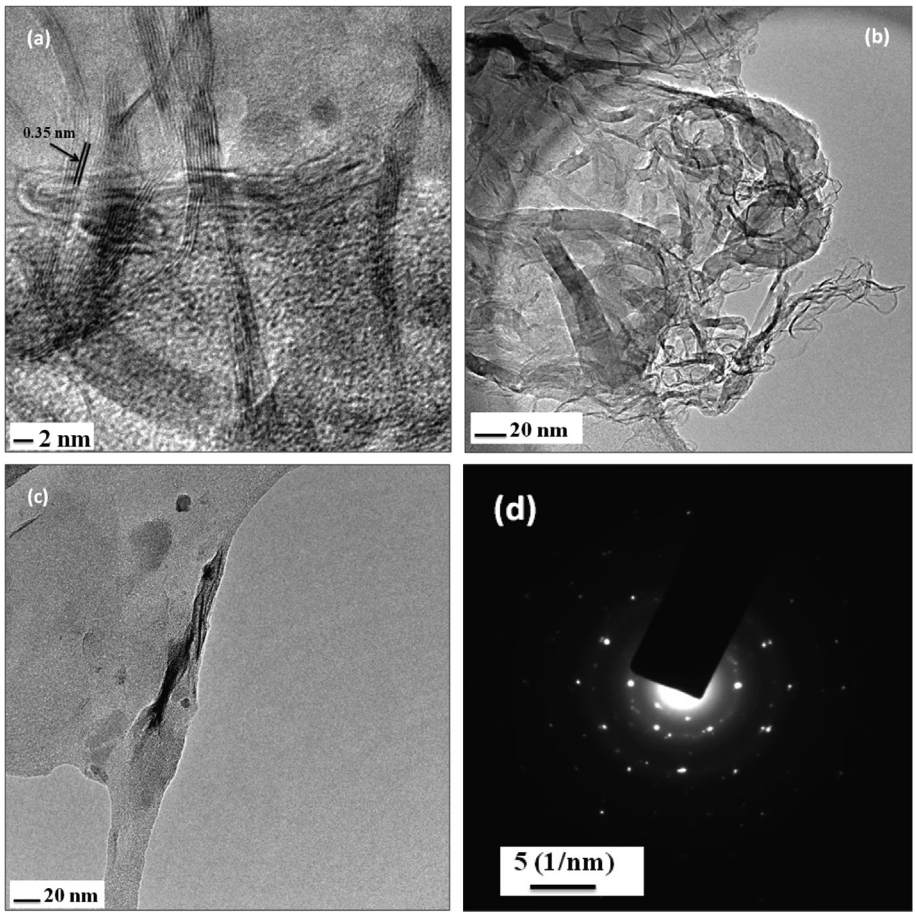


**Fig. 8.** TEM image in (a) showing fringes and no. of layer, (b) multilayer and folded structure of GO, (c) dispersed GO and (d) SAED pattern.

compared to conventional carbon fiber epoxy composites (Fig. 12(a)). This shows that GO addition results in increases in modulus of composite (Fig. 11(b)). The young modulus increases till 0.3 wt% GO and maximum is 35 GPa. Therefore, modulus decreases continuously with increasing the GO content. At 0.6 wt% of GO, modulus is 28 GPa which is higher than conventional carbon fiber-epoxy composites. Fig. 12(a) is depicting the load-displacement curve of the hybrid composites. It is found that addition of GO up to 0.3 wt%, mode of failure can help in more energy dissipation as compared to without GO based composites. In case GO based hybrid composites, elongation of composite decreases, this is due to increase in interfacial interaction with surface functional group of graphene oxide, epoxy resin and carbon fiber. The graphene oxide dispersed in the matrix can be settled with the surface of carbon fiber, which can lead to the formation of a strong bond at the interface of fiber-matrix. These bonds and GO are responsible for stress distribution.

The carbon fiber T-300 used in all composites consist of functional groups on the surface since the fiber only heat heated to 1200 °C during carbon fiber production. So the GO functional groups are utilized for improving interfacial bonding between CF and epoxy matrix. The FTIR data of GO based composites has been used to explain the interaction of GO with epoxy polymer and CF in the composites.

The FTIR result of carbon fiber confirms the presence of oxygeneous functional group on the surface of carbon fiber. In Fig. 9(a),

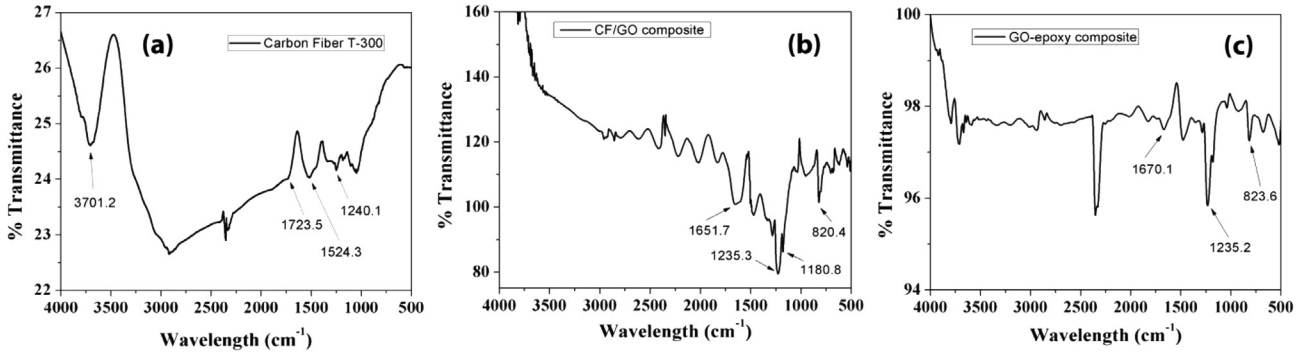


**Fig. 9.** FTIR spectra of (a) carbon fiber, (b) carbon fiber/GO-epoxy composite (c) GO-epoxy composite.

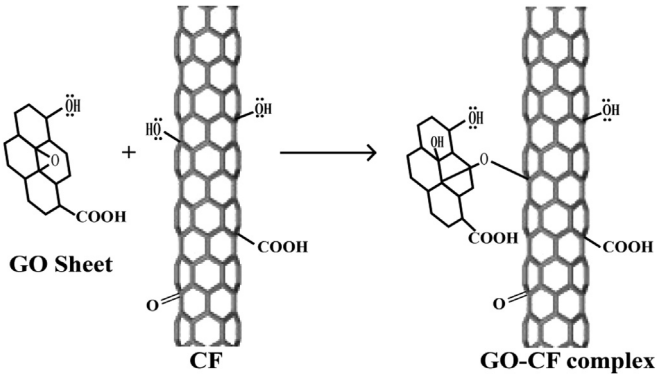


**Fig. 10.** Schematic reaction mechanism between GO and CF resulted in binding with ether bond.

the peaks at 3701.2 $cm^{-1}$ shows the non H-bonded hydroxyl group and O–H group attached with carboxylic group. The peaks at 2930 $cm^{-1}$, 1730 $cm^{-1}$ and 1230 $cm^{-1}$ of symmetric stretching C–H, C═O and C–O bond respectively. The position and intensity peaks notice in CF has been changed in CF/GO-epoxy composite. The hydroxyl group of CF attached with epoxy of GO-epoxy composite resulted in vinyl ether bond between CF and GO. To confirm the nature of bond formed between GO and CF in composite, we have taken the FTIR spectra of CF/GO-epoxy. The ether bond formation is confirmed using FTIR plot of CF/GO-epoxy composite (Fig. 9(b)). In Fig. 9(b), the peak at 1235.2 $cm^{-1}$ and 820.4 $cm^{-1}$ are confirming the presence of asymmetric stretching mode and symmetric stretching mode for C–O bond in vinyl ether respectively. Apart from this, we have observed the shifting of carbonyl peak of GO (Fig. 9(b)) in composite from carbonyl peak of GO (Fig. 2) to lower frequency because of H-bond formation with hydroxyl group of epoxy polymer. The carbonyl peak is observed at 1651.7 $cm^{-1}$ for the GO based CF composites while in case of as such GO carbonyl peak was notice at 1735.6 $cm^{-1}$. This shifting of carbonyl peak is a result of H-bonding between GO and epoxy polymer which lower the bond strength of carbonyl bond resulted in shifting in a peak [56].

To observe the bonding between GO and epoxy resin, the FTIR spectrum of GO-epoxy polymer composite was taken (Fig. 9(c)). It is observed that asymmetric mode of stretching at 1235.2 $cm^{-1}$ and symmetric mode of stretching at 823.6 $cm^{-1}$ of vinyl ether bond. The shifting in carbonyl peak of GO in composite as compared with as such GO is observed. In GO, the carbonyl peak is observed at 1735 $cm^{-1}$ which has shifted to lower frequency in case of GO-epoxy composite i.e., at 1670.1 $cm^{-1}$. This result attributed to the H-bonding between GO and epoxy polymer which lowered the carbonyl bond constant value as observed in Fig. 9(b) [56]. It is also observed the symmetric stretch of N–H and O–H bond between the ranges of 3500–3800 $cm^{-1}$.

In CF/GO-epoxy composite, the surface roughness of carbon fibers are playing very important role in improvement of mechanical properties of hybrid composites. The O–H groups of CF attack at epoxy carbon of GO resulted in opening of strain ring. The schematic reaction mechanism between CF and GO has shown in Fig. 10. The formation of ether bond confirms the chemical bonding between these two. All the above explanation the conform result of chemical bond between GO and CF along with H-bonding between GO and epoxy polymer.

According to Lee et al. [57] graphene modulus is around 1.0 TPa and intrinsic strength ~130 GPa. However, even though modulus and tensile strength decreases to some extent of graphene oxide. It can provide substantial increases in stiffness and strength of the fiber-matrix interface in hybrid composites. This can offer better stress distribution around the fiber-matrix surrounding resin leading to much higher bending strength. On the other hand, higher concentration of GO is not so much effective. Thus there is a percolation threshold of 0.3 wt% of GO that of epoxy resin. The improvement in the properties of composites is due to the crack deflection and crack branching induced by the presence of GO in the matrix which having a high surface area, more energy absorption capacity by the high strength GO. Also, it reveals from SEM micrographs (Fig. 13) GO adhere with carbon fiber surface and GO almost fail in one plane with fibers, this result in brittle type load-displacement behavior.

The mechanical properties of carbon fiber reinforced polymer composites also depends upon the interfacial interaction of fiber and epoxy matrix. Interlaminar shear strength (ILSS) is the one of the best desirable measurement for finding out the interfacial interactions. In Fig. 12(b), depicted the ILSS of hybrid composites with increasing weight% of GO is in epoxy resin. It is observed that increasing weight% of GO and reached maximum for 0.3 wt% GO to epoxy weight. Fig. 12(b) is showing a 23% improvement in the ILSS of 0.3 wt% GO epoxy/carbon fiber composite to pure epoxy/carbon fiber composites. This improved ILSS attributes in fact, that GO contains the oxygeneous function group which exerts polarity onto the surface and edge of GO because of this it exerts good dispersion which lead effective bonding between GO and matrix. Epoxy (Bisphenol A epoxy resin) contains epoxy and hydroxyl as functional group so hydrogen bonding involved among GO molecules and epoxy as well with carbon fibers. As a result good interfacial adhesion with epoxy comes into play resulting in “interlock effect”.

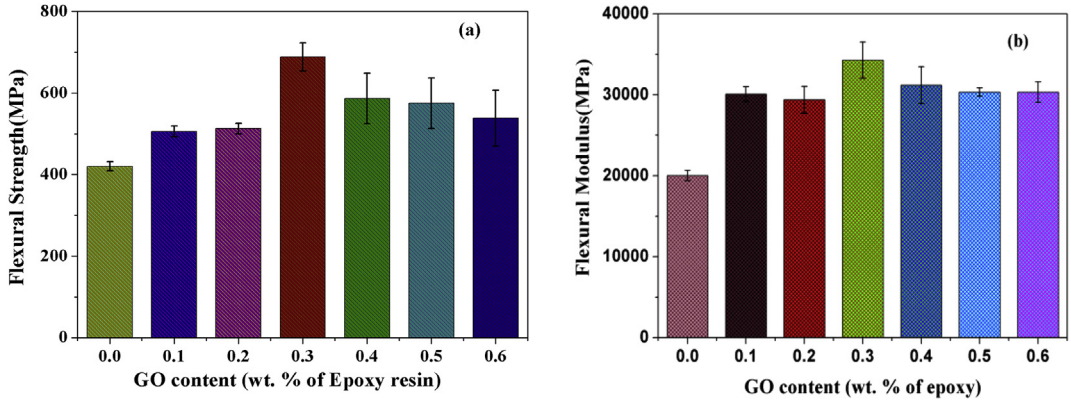


**Fig. 11.** Variation in (a) Flexural strength and (b) Modulus with increasing GO content in epoxy resin.

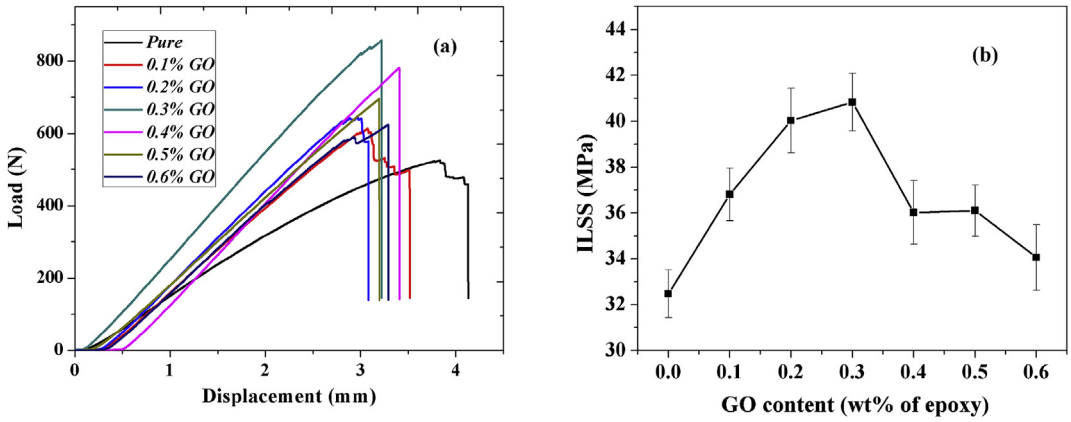


**Fig. 12.** (a) Maximum load vs. extension with GO weight % variation and (b) ILSS variation with GO weight % of epoxy.

This is also due to wrinkled structure GO which induce mechanical interlocking between GO and epoxy matrix [58].

Dispersion of GO at 0.3 wt% was good, but above its concentration it started aggregating. So the aggregation of GO increases with increasing the content of GO above 0.3 wt%. The detrimental effect of GO on shear strength is more after 0.4 wt% GO addition and its increases as we add more GO content in epoxy. We have observed decrement of the ILSS from 40.8 MPa to 36.0 MPa in case 0.3 wt% GO to 0.4 wt% GO content respectively. So 11.7% ILSS reduction from highest ILSS value observed in case of 0.4 wt% GO content and this ILSS deterioration comes from many factors like dispersion of GO into epoxy, agglomeration and undesired bonding of GO with a sizing agent [59]. The agglomeration of GO related to the extra addition of GO from limited amount. GO involved in binding with hardener TETA used so more GO content bind with more TETA molecule resulting in weakness in bonding between epoxy and TETA molecules. So a less molecule of TETA remained for bonding with epoxy. Cross-linking extent between matrix and hardener weakened interfacial interaction between GO, epoxy and fiber. As a consequence decreases in ILSS of composites at higher content of GO. The fracture surfaces of bending tested specimens of different composites were examined. The present investigation results are compared with GO incorporated or GO coated glass and carbon fiber composites available in literature [60–62].

Fei li et al. [60] reported improvement of polyethersulfone (PES) special engineering thermoplastic by incorporating short carbon fiber (SCF) and graphene oxide (GO). In this study, composites were prepared by extrusion compounding and injection molding from the mixture of 12.5 wt% SCF with varying the GO coating content from 0 to 1.0 wt%. The pure PES composite have tensile strength 89 MPa and that of SCF-PES composites 106 MPa. After incorporating GO- in SCF-PES composite, tensile strength increases to 119 MPa at 0.5 wt% GO content. The flexural strength and modulus of pure PES is 126 MPa and 2.56 GPa while that of SCF-PES composite flexural strength and modulus increases to 157 MPa and 4.93 GPa. On the other hand, on incorporation of GO in SCF-PES composites, flexural strength and modulus increases to 182.5 MPa and 6.4 GPa respectively. It is reported that, pure PES in ductile material with the yield point, while SCF-PES composites showing the brittle behavior. The brittle behavior of SCF-PES composites is increases as GO content increases in SCF-PES composites. The enhancement of mechanical properties due to the fact that, the interfacial bonding between SCF and PES has been enhanced by the GO treatment on SCF surface and thus there is better load transfer from PES to the SCF. This result is associated with the fact that interfacial bonding between SCFs and PES is enhanced by the GO treatment on SCF surfaces.

The properties of short carbon fiber composites are not that high as compared to continuous carbon fiber composites and as results this type of composites cannot be used for structural applications.

Mahmood et al. [61], have reported the effect of surface treatment of GO on unidirectional glass fiber (GF) epoxy composite. In this GO was deposited on GF through electrophoretic deposition (EPD) technique, EPD was carried out at various applied voltages up to 10 V/cm with constant deposition time so that homogenous deposition of GO can be achieved on GFs. In case of untreated GF-epoxy composite, tensile strength and inter laminar shear strength (ILSS) is 1475 MPa and 5.7 MPa. While this value of tensile strength and ILSS increases to 1844 MPa and 18.2 MPa in case of GO coated GF-epoxy composite at 10 V/cm applied voltage. There is an improvement of 25% in tensile strength and 219% in ILSS is registered. The improvements in the properties are due to the facts that

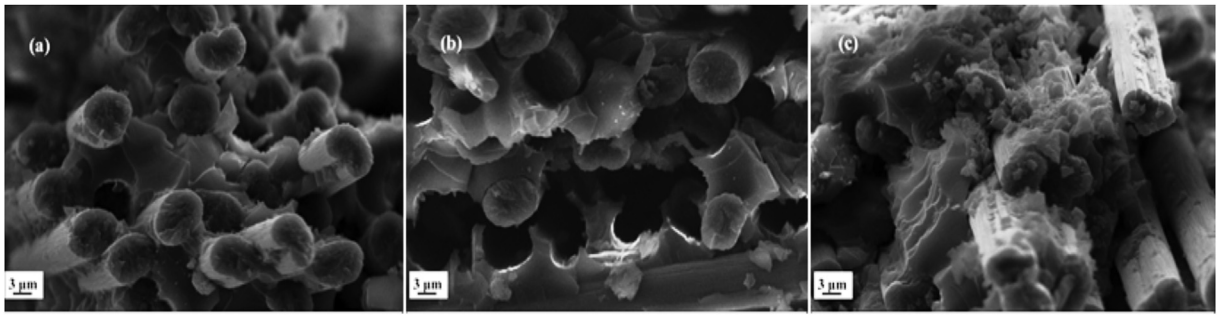


**Fig. 13.** SEM images (a) pure epoxy carbon fiber composite (b) 0.3% GO- epoxy carbon fiber composite (c) 0.6% GO- epoxy carbon fiber composite.

GO creates a favorable bond between GFs and epoxy resin which enhance the effective distribution of load on the GF. The mechanical interlocking is take place between GF and Epoxy resin due to the increase in surface roughness of GF by Go coating.

Park et al. [62], focused on improvement interfacial properties of unidirectional GF- epoxy matrix composites by using novel layer-by-layer (LbL) assembly for the surface modification of the GF. In this case initially glass fiber was coated with GO and then aramid nanofibers (ANF) to improve interfacial properties. The GF-epoxy matrix composite possess interfacial shear strength (IFSS) 20.74 MPa and surface free energy (SFE) 39.33 mN/m. While after uniform GO and ANF coated glass fiber-epoxy composite, IFSS and increases to28.86 MPa and SFE to 44.63 mN/m respectively. The improvement in interfacial properties of GF- epoxy matrix composite is associated with the LbL assembly which facilitates the development of the assembly of multidirectional nanomaterials without significant phase aggregation and controlled architecture among the layers.

The above quoted [60–62] research work has mainly focused on surface modification of either unidirectional carbon fiber or glass fiber using graphene oxide. In our research work, we have used very simple method of introduction GO into epoxy resin and improved the interfacial properties between 2D carbon fiber fabric and epoxy matrix. The introduction of GO into epoxy matrix not only affecting the epoxy matrix surface using H-bonding but also binding with carbon fiber with chemical bond during curing process. In this we have used simple mixing of GO synthesized in laboratory, into the epoxy and fabrication on carbon fiber composite, resulting in significant improvement in mechanical properties of hybrid 2D composites i.e., bending strength, modulus and ILSS by 66,70 and 25% at only 0.3 wt% incorporation of GO. So all the our experiments were associated with cost saving, light weight, minimum used of carbon fibers (45 wt%) and time saving process along with very conventional method GO incorporation.

Fig. 13 are showing the fracture surface of composites observed by SEM. It is evident from Fig. 13(a, b and c) that fiber pulls out was observed in all three types of composites. Among the three, without GO based composites, it failed predominantly by pull out as a result of higher displacement take place in this case, while in case of 0.3 wt% GO based composites extent of pull out is less and composites fail almost in a single plane as a result of the decrease in displacement but the higher load bearing capacity of composites. The higher extent of GO reduced the interfacial interaction, but pull out is not that extent while the fiber surface are rough as a result interactions are quite strong as compared without GO based composites. The fracture behavior is in agreement with load-displacement curve.

## 4. Conclusions

The carbon fiber-graphene oxide epoxy resin based composites demonstrate the excellent mechanical properties on inclusion of GO in an epoxy matrix. The bending strength increases by 66% and modulus by - 70% at only 0.3 wt% of GO. The interlaminar shear strength increases by 25%. The increase in mechanical properties is due to the improvement in properties of epoxy resin and interfacial interaction between reinforcement and matrix by hydrogen bonding and mechanical interlocking of graphene oxide as well. The high surface area of nanosize GO makes better bonding around the reinforcements at the very small content of GO and higher content of GO results in to the agglomeration in the matrix phase which ultimately around the fibers. The graphene oxide utilization is one of the approaches for improving the properties of carbon fiber polymer composites.

## Acknowledgment

Authors are highly grateful to Director, CSIR-NPL, and Head, Advanced Materials and Devices Division, for his kind permission to publish the results. Authors are like to thanks Dr. R. P. Pant, for providing XRD spectra, Ms. Shaveta Sharma for Raman and Mechanical Testing and Mr. Jai Tawale for providing in SEM characterization composites. Authors are also thankful to Mr. Brij Kishore (IISc Banglore) for NMR and Mr. Ashesh Mahto for TEM characterization. One of the author, Abhishek K. Pathak would like to thanks University grant Commission JRF fellowship. Authors also thank DST, for India-Japan International collaborative project funding.

## References

[1] A. Argon, R. Cohen, Toughenability of polymers, Polymer 44 (19) (2003) 6013–6032.
[2] A.C. Garg, Y.-W. Mai, Failure mechanisms in toughened epoxy resins—a review, Compos. Sci. Technol. 31 (3) (1988) 179–223.
[3] E.G. Koricho, G. Belingardi, A.T. Beyene, Bending fatigue behavior of twill fabric E-glass/epoxy composite, Compos. Struct. 111 (2014) 169–178.
[4] K. Friedrich, Z. Lu, A. Hager, Recent advances in polymer composites' tribology, Wear 190 (2) (1995) 139–144.
[5] M. Cirino, K. Friedrich, R. Pipes, Evaluation of polymer composites for sliding and abrasive wear applications, Composites 19 (5) (1988) 383–392.
[6] R.D. Jamison, K. Schulte, K.L. Reifsnider, W.W. Stinchcomb, Characterization and analysis of damage mechanisms in tension-tension fatigue of graphite/epoxy laminates, Eff. Defects Compos. Mater. (1984) 21–55.
[7] J. Degrieck, W. Van Paepegem, Fatigue damage modeling of fibre-reinforced composite materials: review, Appl. Mech. Rev. 54 (4) (2001) 279–300.
[8] J.P. Davim, P. Reis, Study of delamination in drilling carbon fiber reinforced plastics (CFRP) using design experiments, Compos. Struct. 59 (4) (2003) 481–487.
[9] N. Choi, A. Kinloch, J. Williams, Delamination fracture of multidirectional carbon-fiber/epoxy composites under mode I, mode II and mixed-mode I/II loading, J. Compos. Mater. 33 (1) (1999) 73–100.
[10] S. Chand, Review carbon fibers for composites, J. Mater. Sci. 35 (6) (2000) 1303–1313.
[11] A. Mouritz, Review of z-pinned composite laminates, Compos. Part A Appl. Sci. Manuf. 38 (12) (2007) 2383–2397.
[12] L.K. Jain, Y.-W. Mai, On the effect of stitching on mode I delamination toughness of laminated composites, Compos. Sci. Technol. 51 (3) (1994) 331–345.
[13] S.J. Hollister, Porous scaffold design for tissue engineering, Nat. Mater. 4 (7) (2005) 518–524.
[14] M. Delamar, G. Desarmot, O. Fagebaume, R. Hitmi, J. Pinsonc, J.-M. Savéant, Modification of carbon fiber surfaces by electrochemical reduction of aryl diazonium salts: application to carbon epoxy composites, Carbon 35 (6) (1997) 801–807.
[15] F. Severini, L. Formaro, M. Pegoraro, L. Posca, Chemical modification of carbon fiber surfaces, Carbon 40 (5) (2002) 735–741.
[16] P. Allongue, M. Delamar, B. Desbat, O. Fagebaume, R. Hitmi, J. Pinson, J.-M. Savéant, Covalent modification of carbon surfaces by aryl radicals generated from the electrochemical reduction of diazonium salts, J. Am. Chem. Soc. 119 (1) (1997) 201–207.
[17] A. Arbelaiz, B. Fernandez, J. Ramos, A. Retegi, R. Llano-Ponte, I. Mondragon, Mechanical properties of short flax fibre bundle/polypropylene composites: influence of matrix/fibre modification, fibre content, water uptake and recycling, Compos. Sci. Technol. 65 (10) (2005) 1582–1592.
[18] K. Mimura, H. Ito, H. Fujioka, Improvement of thermal and mechanical properties by control of morphologies in PES-modified epoxy resins, Polymer 41 (12) (2000) 4451–4459.
[19] F.H. Gojny, M.H. Wichmann, B. Fiedler, W. Bauhofer, K. Schulte, Influence of nano-modification on the mechanical and electrical properties of conventional fibre-reinforced composites, Compos. Part A Appl. Sci. Manuf. 36 (11) (2005) 1525–1535.
[20] X. Kornmann, M. Rees, Y. Thomann, A. Necola, M. Barbezat, R. Thomann, Epoxy-layered silicate nanocomposites as matrix in glass fibre-reinforced composites, Compos. Sci. Technol. 65 (14) (2005) 2259–2268.
[21] S. Marras, A. Tsimpliaraki, I. Zuburtikudis, C. Panayiotou, Morphological, thermal, and mechanical characteristics of polymer/layered silicate nanocomposites: the role of filler modification level, Polym. Eng. Sci. 49 (6) (2009) 1206–1217.
[22] X. He, F. Zhang, R. Wang, W. Liu, Preparation of a carbon nanotube/carbon fiber multi-scale reinforcement by grafting multi-walled carbon nanotubes onto the fibers, Carbon 45 (13) (2007) 2559–2563.
[23] E. Moaseri, M. Karimi, M. Maghrebi, M. Baniadam, Fabrication of multi-walled carbon nanotube–carbon fiber hybrid material via electrophoretic deposition followed by pyrolysis process, Compos. Part A Appl. Sci. Manuf. 60 (2014) 8–14.

[24] T.-W. Chou, L. Gao, E.T. Thostenson, Z. Zhang, J.-H. Byun, An assessment of the science and technology of carbon nanotube-based fibers and composites, Compos. Sci. Technol. 70 (1) (2010) 1–19.
[25] J. Jyoti, S. Basu, B.P. Singh, S. Dhakate, Superior mechanical and electrical properties of multiwall carbon nanotube reinforced acrylonitrile butadiene styrene high performance composites, Compos. Part B Eng. 83 (2015) 58–65.
[26] S. Aldajah, Y. Haik, Transverse strength enhancement of carbon fiber reinforced polymer composites by means of magnetically aligned carbon nanotubes, Mater. Des. 34 (2012) 379–383.
[27] E. Bekyarova, E.T. Thostenson, A. Yu, M.E. Itkis, D. Fakhrutdinov, T.-W. Chou, R.C. Haddon, Functionalized single-walled carbon nanotubes for carbon fiber-epoxy composites, J. Phys. Chem. C 111 (48) (2007) 17865–17871.
[28] T. Ogasawara, Y. Ishida, T. Kasai, Mechanical properties of carbon fiber/fullerene-dispersed epoxy composites, Compos. Sci. Technol. 69 (11) (2009) 2002–2007.
[29] U. Tayfun, Y. Kanbur, U. Abaci, H.Y. Guney, E. Bayramli, Mechanical, flow and electrical properties of thermoplastic polyurethane/fullerene composites: effect of surface modification of fullerene, Compos. Part B Eng. 80 (2015) 101–107.
[30] M.M. Shokrieh, A.R. Kefayati, M. Chitsazzadeh, Fabrication and mechanical properties of clay/epoxy nanocomposite and its polymer concrete, Mater. Des. 40 (2012) 443–452.
[31] Y. Xu, S. Van Hoa, Mechanical properties of carbon fiber reinforced epoxy/clay nanocomposites, Compos. Sci. Technol. 68 (3) (2008) 854–861.
[32] G. Vaganov, V. Yudin, J. Vuorinen, E. Molchanov, Influence of multiwalled carbon nanotubes on the processing behavior of epoxy powder compositions and on the mechanical properties of their fiber reinforced composites, Polym. Compos. 37 (8) (2016) 2377–2383.
[33] S. Stankovich, D.A. Dikin, G.H. Dommett, K.M. Kohlhaas, E.J. Zimney, E.A. Stach, R.D. Piner, S.T. Nguyen, R.S. Ruoff, Graphene-based composite materials, Nature 442 (7100) (2006) 282–286.
[34] J. Ruan, X. Wang, Z. Yu, Z. Wang, Q. Xie, D. Zhang, Y. Huang, H. Zhou, X. Bi, C. Xiao, Enhanced physiochemical and mechanical performance of chitosan-grafted graphene oxide for superior osteoinductivity, Adv. Funct. Mater. 26 (7) (2015) 1085–1097.
[35] M. Zhang, Y. Wang, L. Huang, Z. Xu, C. Li, G. Shi, Multifunctional pristine chemically modified graphene films as strong as stainless steel, Adv. Mater. 27 (42) (2015) 6708–6713.
[36] S.J. Woltornist, J.-M.Y. Carrillo, T.O. Xu, A.V. Dobrynin, D.H. Adamson, Polymer/pristine graphene based composites: from emulsions to strong, Electr. Conduct. Foams Macromol. 48 (3) (2015) 687–693.
[37] H. Pang, C. Chen, Y.-C. Zhang, P.-G. Ren, D.-X. Yan, Z.-M. Li, The effect of electric field, annealing temperature and filler loading on the percolation threshold of polystyrene containing carbon nanotubes and graphene nanosheets, Carbon 49 (6) (2011) 1980–1988.
[38] P. Song, Z. Cao, Y. Cai, L. Zhao, Z. Fang, S. Fu, Fabrication of exfoliated graphene-based polypropylene nanocomposites with enhanced mechanical and thermal properties, Polymer 52 (18) (2011) 4001–4010.
[39] X. Zhang, X. Fan, C. Yan, H. Li, Y. Zhu, X. Li, L. Yu, Interfacial microstructure and properties of carbon fiber composites modified with graphene oxide, ACS Appl. Mater. Interfaces 4 (3) (2012) 1543–1552.
[40] W.S. Hummers Jr., R.E. Offeman, Preparation of graphitic oxide, J. Am. Chem. Soc. 80 (6) (1958), 1339–1339.
[41] Y. Zhu, S. Murali, W. Cai, X. Li, J.W. Suk, J.R. Potts, R.S. Ruoff, Graphene and graphene oxide: synthesis, properties, and applications, Adv. Mater. 22 (35) (2010) 3906–3924.
[42] D.R. Dreyer, S. Park, C.W. Bielawski, R.S. Ruoff, The chemistry of graphene oxide, Chem. Soc. Rev. 39 (1) (2010) 228–240.
[43] D.C. Marcano, D.V. Kosynkin, J.M. Berlin, A. Sinitskii, Z. Sun, A. Slesarev, L.B. Alemany, W. Lu, J.M. Tour, Improved synthesis of graphene oxide, ACS Nano 4 (8) (2010) 4806–4814.
[44] E. Breitmaier, W. Voelter, Carbon-13 NMR Spectroscopy, 1987.
[45] A. Lerf, H. He, M. Forster, J. Klinowski, Structure of graphite oxide revisited, J. Phys. Chem. B 102 (23) (1998) 4477–4482.
[46] H.-K. Jeong, Y.P. Lee, R.J. Lahaye, M.-H. Park, K.H. An, I.J. Kim, C.-W. Yang, C.Y. Park, R.S. Ruoff, Y.H. Lee, Evidence of graphitic AB stacking order of graphite oxides, J. Am. Chem. Soc. 130 (4) (2008) 1362–1366.
[47] G. Wang, X. Sun, C. Liu, J. Lian, Tailoring oxidation degrees of graphene oxide by simple chemical reactions, Appl. Phys. Lett. 99 (5) (2011) 053114.
[48] Y. Song, S. Li, G. Zhai, J. Shi, Q. Guo, L. Liu, Z. Xu, J. Wang, Mechanical and physical properties of MWCNT/carbon composites with matrix derived from mesocarbon microbeads, Carbon 46 (7) (2008) 1100–1102.
[49] J. Titantah, D. Lamoen, sp 3/sp 2 characterization of carbon materials from first-principles calculations: X-ray photoelectron versus high energy electron energy-loss spectroscopy techniques, Carbon 43 (6) (2005) 1311–1316.
[50] T. Livneh, T.L. Haslett, M. Moskovits, Distinguishing disorder-induced bands from allowed Raman bands in graphite, Phys. Rev. B 66 (19) (2002) 195110.
[51] F. Tuinstra, J.L. Koenig, Raman spectrum of graphite, J. Chem. Phys. 53 (3) (1970) 1126–1130.
[52] M. Pimenta, G. Dresselhaus, M.S. Dresselhaus, L. Cancado, A. Jorio, R. Saito, Studying disorder in graphite-based systems by Raman spectroscopy, Phys. Chem. Chem. Phys. 9 (11) (2007) 1276–1290.
[53] F.A. de La Cruz, J. Cowley, Structure of Graphitic Oxide, 1962.
[54] N.R. Wilson, P.A. Pandey, R. Beanland, R.J. Young, I.A. Kinloch, L. Gong, Z. Liu, K. Suenaga, J.P. Rourke, S.J. York, Graphene oxide: structural analysis and application as a highly transparent support for electron microscopy, ACS Nano 3 (9) (2009) 2547–2556.
[55] S. Dhakate, O. Bahl, Effect of carbon fiber surface functional groups on the mechanical properties of carbon–carbon composites with HTT, Carbon 41 (6) (2003) 1193–1203.
[56] P. Yang, X. Wang, H. Fan, Y. Gu, Effect of hydrogen bonds on the modulus of bulk polybenzoxazines in the glassy state, Phys. Chem. Chem. Phys. 15 (37) (2013) 15333–15338.
[57] C. Lee, X. Wei, J.W. Kysar, J. Hone, Measurement of the elastic properties and intrinsic strength of monolayer graphene, Science 321 (5887) (2008) 385–388.
[58] H. Yang, C. Shan, F. Li, Q. Zhang, D. Han, L. Niu, Convenient preparation of tunably loaded chemically converted graphene oxide/epoxy resin nanocomposites from graphene oxide sheets through two-phase extraction, J. Mater. Chem. 19 (46) (2009) 8856–8860.
[59] L. Chen, S. Chai, K. Liu, N. Ning, J. Gao, Q. Liu, F. Chen, Q. Fu, Enhanced epoxy/silica composites mechanical properties by introducing graphene oxide to the interface, ACS Appl. Mater. Interfaces 4 (8) (2012) 4398–4404.
[60] F. Li, Y. Liu, C.-B. Qu, H.-M. Xiao, Y. Hua, G.-X. Sui, S.-Y. Fu, Enhanced mechanical properties of short carbon fiber reinforced polyethersulfone composites by graphene oxide coating, Polymer 59 (2015) 155–165.
[61] H. Mahmood, M. Tripathi, N. Pugno, A. Pegoretti, Enhancement of interfacial adhesion in glass fiber/epoxy composites by electrophoretic deposition of graphene oxide on glass fibers, Compos. Sci. Technol. 126 (2016) 149–157.
[62] B. Park, W. Lee, E. Lee, S.H. Min, B.-S. Kim, Highly tunable interfacial adhesion of glass fiber by hybrid multilayers of graphene oxide and aramid nanofiber, ACS Appl. Mater. Interfaces 7 (5) (2015) 3329–3334.